Int. J. Mech. Sci. Vol. 29, No. 7, pp. 507–524, 1987
Printed in Great Britain.

0020–7403/87 $3.00 + .00

TOWARDS A NEW THEORY OF COLD ROLLING THIN FOIL

N. A. FLECK and K. L. JOHNSON
University Engineering Department, Trumpington Street, Cambridge CB2 1PZ, U.K.

(*Received* 10 *October* 1986)

Abstract—The theoretical framework is developed for a new theory of cold rolling thin metallic foil. Unlike previous theories, the work rolls are allowed to deform to a non-circular profile and finite regions of no-slip between strip and work rolls are allowed to occur in the roll bite. The theory predicts that plastic reduction occurs near entry and near exit of the roll bite, separated by a central region where the strip does not suffer reduction and does not slip relative to the work rolls. As the reduction is decreased to zero the theory reduces to essentially the Johnson and Bentall theory [*J. Mech. Phys. Solids* **17**, 253 (1969)] for the onset of plastic reduction in a strip. At large strip thicknesses and finite reductions the new theory approximates the Bland and Ford theory [*Proc. Inst. Mech. Engrs* **159**, 144 (1948)] of cold rolling.

NOTATION

a contact width from centre line of rolls to entry or exit location
b semi-thickness of strip
$\Delta b_1 = b_0 - b_1$ reduction in semi-thickness of strip from entry of roll bite to central, elastic no-slip zone
$\Delta b_2 = b_0 - b_2$ reduction in semi-thickness of strip from entry to exit of roll bite
p, q normal pressure and shear stress, respectively, between strip and work rolls
$p_0 = E_R^* a_0/2R$ maximum Hertzian pressure
$r = (b_0 - b_2)/b_0$ overall reduction of strip
$r_1 = (b_1 - b_2)/b_1$ intermediate reduction of strip
$\dot{s} = v_S - v_R$ slip velocity
u, w tangential and normal displacements in the x and z directions, respectively
v absolute velocity in x direction
x, z Cartesian co-ordinates
x_A location of boundary between zones A and B
x_B location of boundary between zones B and C
x_C location of boundary between zones C and D
x_D location of boundary between zones D and E
x_E location of boundary between zones E and F
x_F location of boundary between zones F and G
E Young's modulus
$E^* = E/(1-\nu^2)$ Plane strain Young's modulus
E' stiffness constant, where $\dfrac{1}{E'} = \dfrac{(1-2\nu_R)(1+\nu_R)}{E_R} + \dfrac{\nu_S(1+\nu_S)}{E_S}$
$\bar{H} = \dfrac{2b_0 E_R^*}{\mu R Y_S}$ non-dimensional inlet thickness of strip
$K_p = \dfrac{8}{3\pi}\dfrac{E_R^*}{a_0}$ constant of proportionality for pressure in elastic foundation model
$K_q = \dfrac{16}{9\pi}\dfrac{E_R^*}{a_0}$ constant of proportionality for shear stress in elastic foundation model
L_3, L_4, L_5, L_6, L_7 unknown constants
Q rolling torque per work roll, per unit width of strip
$\bar{Q} = \dfrac{Q E_R^{*2}}{R^2 Y_S^3}$ non-dimensional rolling torque
R radius of undeformed work roll
R' radius of deformed work roll
$U = \dfrac{\mu E_R^*}{Y_S}$ dimensionless group
V velocity of unstrained strip or rolls in x direction
W rolling load per unit width of strip
$\bar{W} = \dfrac{W E_R^*}{R Y_S^2}$ non-dimensional rolling load
Y_S yield stress of strip in uniaxial tension

$\alpha_3, \alpha_4, \alpha_5, \alpha_6, \gamma$	parameters used to define stresses in the elastic, non-slip zone
$\varepsilon_x, \varepsilon_z$	tensile strain in longitudinal x direction and normal z direction, respectively
ν	Poisson's ratio
σ_x, σ_z	tensile direct stress in x and z directions, respectively
τ	shear stress
$\xi = (V_S - V_R)/V_R$	creep coefficient
μ	coefficient of Coulomb friction
ω	angular velocity of work rolls

Subscripts

crit	critical
S	strip
R	work roll
0	quantity at entry of strip into roll bite
1	quantity in the central, elastic no-slip zone
2	quantity at exit of strip from roll bite

1. INTRODUCTION

A large tonnage of aluminium and steel foil is cold rolled each year for the packaging and electrical industries. There is no satisfactory rolling theory for this process, as conventional cold rolling models fail when the strip is thinner than about 100 μm. In this paper, the framework for a new theory of rolling thin foil is developed. The theory is novel in the sense that it attempts to model seriously the deformation of the work rolls and the frictional conditions between the work rolls and foil.

2. PREVIOUS THEORIES OF COLD ROLLING

Cold rolling consists of passing a strip of thickness $2b_0$ between two work rolls in order to reduce the strip thickness to a smaller value of $2b_2$, see Fig. 1(a). The overall reduction, r, is given by $(b_0 - b_2)/b_0$. Usually, lubricant is applied between the strip and work rolls in order to reduce the coefficient of Coulomb friction, μ, and thereby to reduce the rolling load.

Conventional theories of cold rolling developed by von Kármán [1], Orowan [2] and Bland and Ford [3] assume that the work rolls remain circular in shape, although the roll radius may be increased from R to R' in the arc of contact due to roll deformation, Fig. 1(a). The theories also assume that limiting Coulomb friction occurs over the whole contact arc

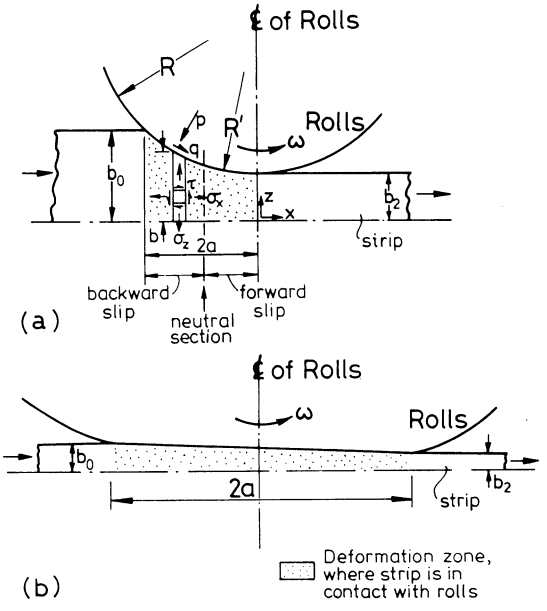

FIG. 1. Cold rolling of (a) thick strip and (b) thin foil.

between work rolls and strip. At entry the strip moves slower than the rolls, while at exit the strip moves faster than the rolls. No-slip between the rolls and strip occurs only at a single section between entry and exit, known as the neutral section. There the strip and rolls have a common velocity of ωR, where ω is the angular velocity of the rolls, Fig. 1(a).

These assumptions about the geometry of the rolls and the slip conditions are reasonable for the case of rolling a thick strip, where the ratio of inlet strip thickness, $2b_0$, to length of contact zone, $2a$, is of the order of unity. When thin foil is rolled, the ratio a/b_0 is much greater than unity, see Fig. 1(b). Then, the rolls are deformed into a non-circular shape and a region of no-slip (neutral zone) may exist at the centre of the contact zone.

With decreasing strip thickness, the roll load required to achieve a given reduction increases and there has been speculation that a 'limiting gauge' may exist below which increasing load results in increasing deformation of the rolls without further plastic reduction in the strip. This behaviour is predicted by the Bland and Ford theory [3] and also by Ford and Alexander [4], who examined the stresses in an elastic strip to determine the load at which yield begins. Their conclusion that a limiting gauge exists arose from their erroneous assumption that slip, and hence limiting friction, exists throughout the contact zone. Johnson and Bentall [5] also examined the problem of first yield and the onset of reduction of thin foil, but admitted the possibility of a central region of no-slip. They showed that a region of no-slip would be expected over a substantial fraction of the contact zone and that, in consequence, no limiting gauge would be reached; a conclusion which is consistent with practice in rolling aluminium foil.

The new theory of foil rolling presented here seeks to extend the analysis of Johnson and Bentall [5] for the case of finite reductions of thin strip. This new theory allows for the existence of a no-slip region, and relaxes the assumption that the deformed work rolls remain circular. It is shown below that the new theory reduces essentially to the Johnson and Bentall solution [5] in the limit of zero reduction, and approximates the Bland and Ford solution [3] for finite reduction of thick strip.

Grimble *et al.* [6, 7] and Quan [8] have also developed new theories of cold rolling. While Grimble and co-workers assume correctly that the work rolls deform to a non-circular profile, they assume mistakenly that limiting friction exists throughout the contact zone. Quan recognizes the existence of a central elastic region but assumes incorrectly that the rolls remain circular.

3. ASSUMPTIONS OF NEW THEORY

The new theory assumes plane deformations with no lateral spread of the strip. For simplicity, zero front and back tensions on the strip are considered; non-zero front and back tensions can be incorporated in a straightforward manner, but make the analysis more cumbersome.

Detailed assumptions are now given about the behaviour of the strip, rolls and the slip conditions at the interface between rolls and strip.

3.1 *Behaviour of strip*

We assume homogeneous deformation of the strip, such that plane sections remain plane. This is justified by considering the equations of equilibrium in non-dimensional form. The stresses in the strip and between the strip and rolls are defined in Fig. 1(a), using the Cartesian co-ordinate system given in the figure. Let the stresses in the strip, σ_x, σ_z and τ be functions of the Cartesian co-ordinates x and z. Then by equilibrium,

$$\frac{\partial}{\partial(z/b_0)}\left(\frac{\tau}{p_0}\right) = -\left(\frac{b_0}{a}\right)\frac{\partial}{\partial(x/a)}\left(\frac{\sigma_x}{p_0}\right)$$

and

$$\frac{\partial}{\partial(z/b_0)}\left(\frac{\sigma_z}{p_0}\right) = -\left(\frac{b_0}{a}\right)\frac{\partial}{\partial(x/a)}\left(\frac{\tau}{p_0}\right), \tag{1}$$

where p_0 is a representative pressure given by the maximum pressure on the strip, $2a$ is the contact length and $2b_0$ is the strip thickness at entry, see Fig. 1(a).

The non-dimensional equilibrium equations (1) indicate that the variation of stress across the thickness of the strip may be neglected when $b_0/a \ll 1$; this condition is met for the case of rolling thin foil.

Now consider an element of the strip, of height $2b$ and length $\mathrm{d}x$, Fig. 1(a). It is assumed that the stresses σ_z and σ_x acting on this element are independent of z, and are principal stresses. Since the interfacial frictional stress on the element, q, is much less than the normal stress, p, in lubricated contact, and $b_0/a \ll 1$, the assumption that σ_x and σ_z are principal stresses (and $\tau = 0$) is justified.

Vertical equilibrium of forces on the element of the strip shown in Fig. 1(a) gives $\sigma_z = -p$, since $\mathrm{d}b/\mathrm{d}x \ll 1$, while horizontal equilibrium leads to,

$$b\frac{\mathrm{d}\sigma_x}{\mathrm{d}x} + (\sigma_x - \sigma_z)\frac{\mathrm{d}b}{\mathrm{d}x} + q = 0. \tag{2}$$

The strip is assumed to behave in an isotropic, elastic–perfectly plastic manner, with a Young's modulus, E_S, and a Poisson's ratio, ν_S. Yield occurs when $|\sigma_z - \sigma_x| = Y_S$, where Y_S is the uniaxial yield stress of the strip, in accordance with the Tresca yield criterion.

Since the strip is much thinner than the elastic deformation of the rolls, we ignore elastic and contained plastic compression of the strip in the z direction. In the zone of contained plastic flow, plastic strains are of elastic order of magnitude, as discussed below.

3.2 *Behaviour of rolls*

An exact treatment of the elastic deformation of the rolls is difficult since the elastic displacements (normal and tangential) of a surface point in the nip are integral functions of the pressure and traction distributions throughout the nip. For the purposes of this exploratory study the problem was simplified by adopting an elastic foundation or 'mattress model' for the deformation of the rolls. In its simplest form the pressure at location x in the nip is related to the normal displacement of the surface of the roll at that point $w(x)$ by

$$p(x) = K_p w(x), \tag{3}$$

where K_p is a constant 'foundation modulus' whose value is chosen to give a good match with the true deformation. Similarly in the tangential direction the interfacial shear traction $q(x)$ is related to the tangential displacement $u(x)$ by

$$q(x) = K_q u(x). \tag{4}$$

Such a relationship is sometimes referred to as the 'wire brush' model, since individual bristles deform independently of their neighbours.

However, the use of equation (3) for the normal deformation of the rolls has an obvious shortcoming. With thin foil the plastic compression of the foil is generally small compared with the elastic compression of the rolls, so that the overall pressure distribution is approximately Hertzian (elliptical). In the limit of zero reduction, examined by Johnson and Bentall [5], it will be exactly so. But the mattress model of equation (3), in the limit of purely elastic deformation, leads to a *parabolic* distribution of pressure. This discrepancy was found to be significant so that the assumed relationship between roll pressure and deformation was modified to

$$p(x) = p_0\sqrt{1 - (x/a_0)^2} - K_p \Delta b, \tag{3a}$$

where p_0 is the maximum pressure and a_0 is the distance from the contact at entry to the centre-line of the rolls. The mattress model is retained for the *perturbation* in the pressure at point x due to the plastic reduction $2\Delta b(x)$ of the foil at that point. Note that equation (3a) reduces to the correct Hertzian form when the plastic reduction is zero.

The choice of values of K_p and K_q is based on comparison with the exact solution of known problems and is discussed by Johnson [9]. On this basis we have taken $K_p = 8E_R^*/3\pi a_0$ and $K_q = \frac{2}{3}K_p$, where E_R^* is the plane strain modulus of the rolls, $E_R/(1 - \nu_R^2)$.

3.3 *Slip behaviour*

The Coulomb friction law is assumed, with $|q| < \mu p$ for no-slip, and $q/\mu p = -\dot{s}/|\dot{s}|$ for slip. Here, $\dot{s}$ is the slip velocity of the strip relative to the rolls at any location.

Let the velocity of the unstrained strip be V_S and the velocity of the unstrained rolls be V_R. Then, the velocity of the strained strip, v_S, is

$$v_S = V_S(1 + (\varepsilon_x)_S), \tag{5}$$

where $(\varepsilon_x)_S$ is the longitudinal strain in the strip. Similarly, the velocity of the surface of the rolls, v_R, is

$$v_R = V_R(1 + (\varepsilon_x)_R) \tag{6}$$

where $(\varepsilon_x)_R$ is the longitudinal strain at the surface of the rolls. The slip velocity, $\dot{s} = v_S - v_R$ is expressed by,

$$\frac{\dot{s}}{V_R} = \frac{v_S - v_R}{V_R} = \frac{V_S}{V_R}(1 + (\varepsilon_x)_S) - (1 + (\varepsilon_x)_R). \tag{7}$$

If we define the creep ratio, ξ, by $(V_S - V_R)/V_R$, then equation (7) reduces to our fundamental equation of slip,

$$\frac{\dot{s}}{V_R} = (\varepsilon_x)_S - (\varepsilon_x)_R + \xi, \tag{8}$$

where we have neglected the second-order quantity $\xi(\varepsilon_x)_S$. In regions of slip $|\dot{s}| > 0$ and $q/\mu p = -\dot{s}/|\dot{s}|$, while in regions of no-slip $\dot{s} = 0$ and $|q| \leqslant \mu p$.

It is known from industrial practice that the roll speed, V_R, has a large influence on the foil rolling process. Usually, an increase of roll speed at a fixed rolling load leads to an increase of the amount of plastic reduction. Unfortunately, the effect of speed is not modelled explicitly by the Coulomb friction law. As a first approximation, an empirical relation between μ and V_R could be determined by matching the new rolling model to mill data. This is not pursued here.

4. GENERAL FEATURES OF THE SOLUTION

The analysis predicts that a number of different zones exist in the roll bite, where the stress state in the strip may be elastic or plastic, and there may be slip or no-slip. Equations for the stresses and deformations of the rolls and strip in each region are given in Appendix 1, while the method of solution is outlined in Appendix 2.

The general form of the solution is shown in Fig. 2. Seven distinct zones exist in the roll bite, labelled A–G. We shall consider the behaviour of the strip in each zone in turn.

Zone A (see Fig. 2)

At entry, zone A, the strip is elastic and travels more slowly than the rolls. Limiting friction acts on the strip, pulling it into the nip. The thickness of the strip remains equal to $2b_0$ since normal elastic compression of the strip is ignored. The normal pressure on the strip, $p(x)$, equals $p_0\sqrt{1-(x/a_0)^2}$ by equation (3a), and the longitudinal stress $\sigma_x(x)$ is derived by integrating equation (2) with $q = \mu p$. The pressure, p, builds up much more quickly with increasing x than does σ_x, and the strip yields at the end of zone A.

Zone B

In zone B, the strip experiences plastic reduction and the thickness decreases by a total amount of $2\Delta b_1$. Since the strip experiences large tensile plastic strains in the x direction while the rolls remain elastic, it is impossible for the slip velocity, $\dot{s}$, to be uniformly at zero from equation (8). Therefore, slip occurs in zone B with $\dot{s} < 0$ and $q = \mu p$. The variation in pressure $p(x)$ through zone B is found by integrating equation (2) numerically, with the aid of equation (3a) and σ_x given by $\sigma_x = Y_S + \sigma_z$.

Zone B ends when there is no more plastic reduction of the strip, that is when $\mathrm{d}b/\mathrm{d}x = 0$. If plastic flow with slip were allowed to continue beyond this point the strip thickness would increase again, which violates the plastic flow rule. Thus, a central region exists where the strip does not experience appreciable plastic reduction. This central region consists of zones C–E. There, the normal pressure is given by $p(x) = p_0\sqrt{1-(x/a_0)^2} - K_p\Delta b_1$, where $2\Delta b_1$ is the

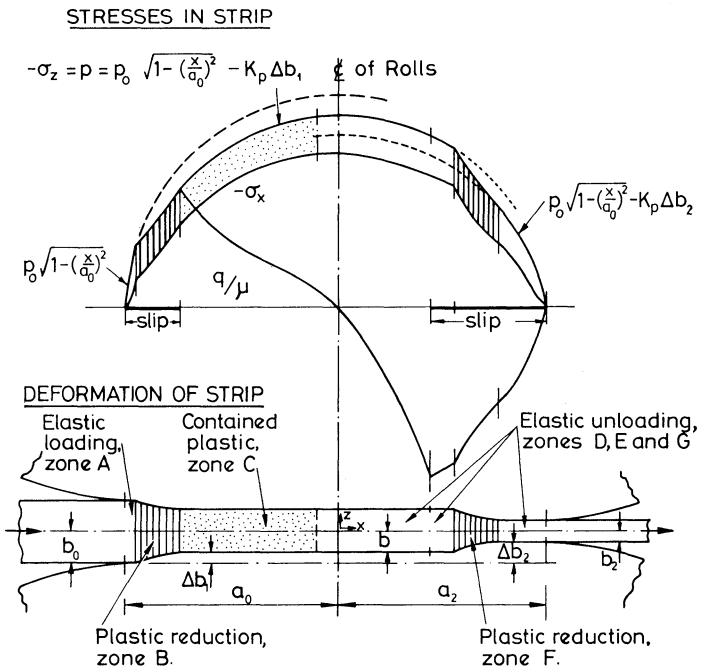

FIG. 2. General solution for stresses in strip and deformation of strip.

reduction of strip thickness in zone B. This pressure distribution is elliptical in shape but is reduced in magnitude by an amount $K_p\Delta b_1$ from the Hertzian solution.

Before further examination of the central zones C–E, we shall consider the deformation state in zones F and G near the exit of the contact region.

Zones F and G

Zone G is adjacent to the exit of the bite. In this zone, the strip is moving faster than the rolls and $q = -\mu p$. The strip behaves elastically and experiences a normal pressure, $p = p_0\sqrt{1-(x/a_0)^2} - K_p\Delta b_2$, where $2\Delta b_2 = r2b_0$ is the total plastic reduction of the strip thickness in the roll bite. The size of the contact region at exit, a_2, is determined by putting $p = 0$, $x = a_2$ and $\Delta b_2 = rb_0$ in equation (3a) and solving for a_2.

We compute the longitudinal stress, σ_x, in zone G by integrating equation (2), with the boundary condition that $\sigma_x = 0$ at $x = a_2$. Since elastic compression in the z direction is neglected for the strip, db/dx equals zero in equation (2). The start of zone G and the end of zone F is found by locating the point in zone G where the yield criterion $|\sigma_x - \sigma_z| = Y_S$ is satisfied.

In zone F, the strip experiences plastic reduction and slips in a forward direction relative to the rolls. The interfacial shear stress q is given by $-\mu p$, while the longitudinal stress, σ_x, equals $\sigma_z + Y_S$, in accordance with the yield criterion. The normal pressure, p, is computed by integrating equation (2) numerically, while making use of the assumption $\sigma_z = -p$, the yield condition and of equation (3a). The boundary between zones E and F is determined by determining the point of intersection of the pressure profile in zone F with the pressure distribution $p = p_0\sqrt{1-(x/a_0)^2} - K_p\Delta b_1$ in zone E.

Zones C, D and E

We now consider the central zones C, D and E where no significant plastic reduction occurs. We have already argued that a slip region with plastic reduction of the strip cannot occur in zone C, adjacent to zone B. Let us consider a number of alternatives to show that the strip suffers contained plastic flow with no slip in zone C, as shown in Fig. 2.

(1) Suppose the strip is elastic, and slip occurs with $q = \mu p$ in zone C. This leads to the rapid build up of a large compressive longitudinal stress σ_x with increasing x, until the strip yields in reverse and thickens! This is incorrect on physical grounds.

(2) Suppose the strip is elastic, but does not slip in zone C. The longitudinal stress σ_x is calculated from equations (2), (3a) and (8). The solution for σ_x indicates that yield is exceeded, violating the yield condition.

(3) Suppose, correctly, that the strip is at yield and no-slip occurs in zone C. The strip experiences further tensile plastic strain in the x direction of elastic order of magnitude, in order to maintain no-slip with the elastically deforming rolls according to equation (8). The longitudinal stress σ_x in the strip is given by the yield condition, $\sigma_x = Y_S + \sigma_z$, and the shear stress q is derived from the equilibrium equation (2). Since the plastic strains in the strip are of elastic order of magnitude in this zone, compression of the strip in the z direction is neglected and $\mathrm{d}b/\mathrm{d}x = 0$ in equation (2). The deformation in this zone may be described as 'contained plastic flow'.

Zone C cannot exist for $x > 0$, since for $x > 0$ equation (8) dictates that additional small *compressive* longitudinal plastic strains are required in order to maintain the no-slip condition. Such compressive plastic strains violate the plastic flow rule. Therefore, zone C is followed by a region D of elastic unloading. In zone D no slip occurs until q/μ reaches $-p$, whereupon the strip slips while remaining elastic. This is zone E.

In region E, the strip moves faster than the rolls and $q = -\mu p$. The longitudinal stress, σ_x, is computed by integrating equation (2), with $\mathrm{d}b/\mathrm{d}x = 0$.

The stresses in zone D are determined by solving equations (2) and (8), assuming no-slip. Full details are given in Appendix 1. The boundaries of zone D are located by matching the stresses in zone D to the stresses in zones C and E, as described in Appendix 2.

The solution illustrated in Fig. 2 is significantly different from previous solutions by Bland and Ford [3]. In the present analysis, the rolls are deformed to a flat profile with a Hertzian pressure distribution, except where significant plastic reduction occurs. The zones of plastic reduction B and F occupy a small fraction of the contact region compared with the central, no-slip zones.

5. CALCULATION OF ROLLING LOAD AND ROLLING TORQUE

The rolling load, W, per unit width of strip and the rolling torque, Q, per work roll, per unit width of strip are calculated by considering the stresses acting on the centre-plane of the strip. Thus,

$$W = \int_{-a_0}^{a_2} p(x)\,\mathrm{d}x \tag{9}$$

and

$$Q = \int_{-a_0}^{a_2} -p(x)x\,\mathrm{d}x. \tag{10}$$

The pressure distribution, size of contact region and the slip distribution ($\dot{s}/V_R$) associated with plastic reduction of the strip can be determined from a knowledge of the solution in zones A, B, F and G. An examination of the equations for these stresses and the slip distribution, as summarized in Appendix 1, shows that only three independent non-dimensional groups, $\mu a_0/b_0$, r and $U = \mu E_R^*/Y_S$ are required in order to determine the non-dimensional rolling load $\bar{W} = WE_R^*/RY_S^2$, non-dimensional rolling torque $\bar{Q} = QE_R^{*2}/R^2Y_S^3$, non-dimensional inlet thickness $\bar{H} = 2b_0E_R^*/\mu RY_S$, total slip at entry $((v_S - v_R)/V_R)_{entry}$, and the total slip at exit $((v_S - v_R)/V_R)_{exit}$. We write this symbolically as,

$$\bar{W}, \bar{Q}, \bar{H}, \left(\frac{v_S - v_R}{V_R}\right)_{entry}, \left(\frac{v_S - v_R}{V_R}\right)_{exit} = f\left(\frac{\mu a_0}{b_0}, r, U\right). \tag{11}$$

For most engineering purposes, equation (11) provides adequate information and the details of the stress distribution within zones C, D and E are not required. Equation (11) can be re-arranged to express $\bar{W}$, $\bar{Q}$ and the slips at entry and exit in terms of $\bar{H}$ rather than $\mu a_0/b_0$,

$$\bar{W}, \bar{Q}, \left(\frac{v_S - v_R}{V_R}\right)_{entry}, \left(\frac{v_S - v_R}{V_R}\right)_{exit} = f(\bar{H}, r, U). \tag{12}$$

We complete the solution by finding the stresses and slip distribution in the central zones C, D and E. For this purpose, two further non-dimensional groups are required, $\mu E_S^*/E_R^*$ and E_S^*/E', where $E_S^* = E_S/(1-\nu_S^2)$ is the plane strain Young's modulus of the strip and $1/E' = ((1-2\nu_R)(1+\nu_R)/E_R) + (\nu_S(1+\nu_S)/E_S)$.

5.1 *Regimes of operation*

A typical plot of $\bar{W}$ vs $\bar{H}$ is given in Fig. 3 for a range of plastic reductions and $U = 30$ (typical for rolling aluminium alloy with steel rolls). Several regimes, corresponding to different stress states in the roll bite, are predicted by the new theory, and are displayed in Fig. 3. The general solution shown in Fig. 2 and discussed above attains limiting states at zero reduction, large reductions and at large strip thicknesses. We shall consider first the solution as r is increased from zero to a high value, and then the solution for large $\bar{H}$ and finite r.

5.2 *Effect of* r *on the stress state in the nip*

Consider a fixed inlet strip thickness, $\bar{H} = 7.5$, and an increasing rolling load, $\bar{W}$, as shown in Fig. 3.

At operating point P_1 in Fig. 3, $\bar{W}$ is sufficiently large to initiate plastic reduction. The plastic zones B and F are of zero width, and the other zones are of finite size. The stress distribution within the nip is given in Fig. 4, for the case where the non-dimensional groups $\mu E_S^*/E_R^*$ and E_S^*/E' are given the values 0.01 and 0.683, respectively. These values are representative for rolling aluminium and its alloys between steel rolls.

An increase in rolling load leads to an increase in plastic reduction until $r = 10\%$ and point P_2 is reached in Fig. 3. The stresses in the strip and the slip velocity of the strip relative to the rolls $(v_S - v_R)/V_R$ are given in Fig. 4. The slip is calculated from the plastic-strain distribution in the strip; details are given in Appendix 1. Figure 4 shows that the size of the plastic zone, the amount of plastic reduction and the magnitude of slip are all greater at entry than at exit. Difficulty was encountered at finding a satisfactory solution for zone D at small reductions. It appears that the model of roll deformation adopted here is unable to predict rapidly changing local distributions of σ_x and q.

When $\bar{W}$ is increased further, point P_3 is reached in Fig. 3 and $r = 30\%$. Again, most of this reduction occurs at entry, which is reflected by the fact that slip at entry is much greater than at exit, Fig. 4.

When the rolling load is increased further a critical value of reduction, r_{crit}, is attained at point P_4 in Fig. 3. This is associated with no yield near the exit of the contact region and zone

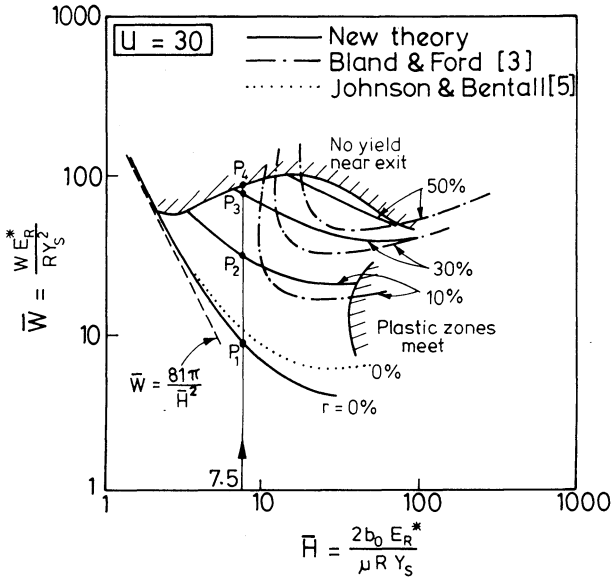

FIG. 3. Predicted rolling load, $\bar{W}$, as a function of inlet strip thickness, $\bar{H}$, and reduction, r. The predictions are compared with previous work of Bland and Ford [3] and Johnson and Bentall [5]. As r is increased at $\bar{H} = 7.5$, the operating points P_1, P_2, P_3 and P_4 are reached.

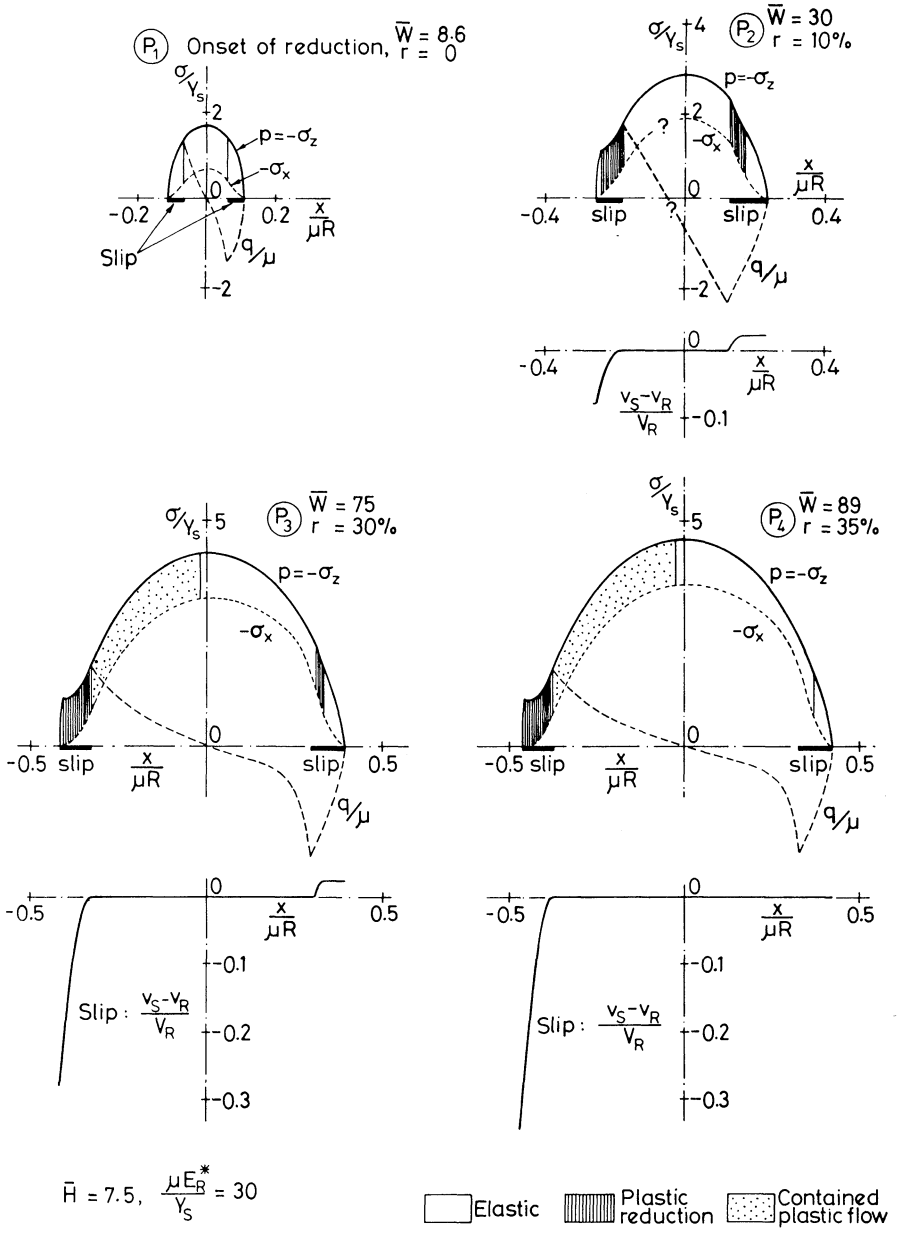

FIG. 4. Distribution of stresses in strip, and slip of strip relative to work rolls. The rolling load, $\bar{W}$, is increased from 8.6 to 89, while keeping $\bar{H}$ constant at 7.5. The operating points P_1, P_2, P_3 and P_4 are defined previously in Fig. 3.

F disappears. Figure 4 shows the stress and slip distributions for $r = r_{crit} = 35\%$ and $\bar{H} = 7.5$. Zones E and G become the same zone, and plastic reduction occurs only at entry.

A further increase in rolling load leads to greater reductions at entry, with no yield near the exit of the contact region. The stress and slip distributions are qualitatively the same as for $r = r_{crit}$, but no precise calculations have been made.

It is clear from Figs 3 and 4 that for a fixed value of $\bar{H}$, an increase of $\bar{W}$ leads to a monotonic increase of r and of the size of the contact region.

5.3 *Case of large* $\bar{H}$

Consider the case where $\bar{H}$ approaches 100 and r is finite in Fig. 3. The analysis suggests that the plastic zones B and F meet and the neutral *region* containing zones C, D and E reduces to a neutral *section* between zones B and F. For these values of $\bar{H}$, the assumption that

$b_0/a_0 \ll 1$ is no longer valid and conventional strip rolling theories are at least as accurate as the present analysis.

6. COMPARISON OF NEW THEORY WITH PREVIOUS WORK

6.1 *Comparison of new theory with the Bland and Ford model*

The predictions of the Bland and Ford model [3] are compared with the new theory in Fig. 3. For $\bar{H}$ in the range 40–100, the two theories show reasonable agreement. This is not surprising since the new theory *predicts* the existence of a neutral section at high $\bar{H}$ values, while the Bland and Ford model *assumes* the existence of a neutral section. The two theories predict slightly different rolling loads as Bland and Ford assume that the deformed rolls remain circular in shape, while we use a hybrid elastic foundation model to account for roll deformations.

At smaller values of $\bar{H}$ the Bland and Ford model fails, since it predicts erroneously high rolling loads and a limiting gauge, Fig. 3.

6.2 *Comparison of new theory with Johnson and Bentall solution for onset of plastic reduction*

The new theory is compared with the Johnson and Bentall solution [5] for the onset of plastic reduction in Fig. 3. The difference in behaviours at large $\bar{H}$ is due to the fact that Johnson and Bentall include the effect of normal elastic deformation of the strip on the contact width, while the new theory ignores this. Both analyses predict that as $\bar{H}$ tends to zero the rolling load $\bar{W}$ is given by $\bar{W} = 81\pi/\bar{H}^2$, independent of U.

7. PRESENTATION OF ROLLING LOAD, TORQUE AND SLIP CURVES

The optimum way of presenting the predicted rolling load, torque and slips at entry and at exit is now discussed. Examination of the dependence of $\bar{W}$, $\bar{Q}$, $((v_S - v_R)/(V_R)_{entry}$ and of $((v_S - v_R)/V_R)_{exit}$ upon $\bar{H}$, r and U, equation (12), shows that the influence of U upon the dependent variables can be reduced if equation (12) is re-written as

$$\bar{W}/U,\ \bar{Q}/U,\ \left(\frac{v_S - v_R}{V_R}\right)_{entry},\ \left(\frac{v_S - v_R}{V_R}\right)_{exit} = f(\bar{H}\sqrt{U},\ r,\ U). \tag{13}$$

Figures 5–7 demonstrate that the non-dimensional groups on the left-hand side of equation (13) depend little upon the independent variable U on the right-hand side of equation (13).

Consider first the plot of $\bar{W}/U$ vs $\bar{H}\sqrt{U}$ shown in Fig. 5, for varying r and U. For $r = 0$, $\bar{W}$ approaches $81\pi/\bar{H}^2$ as $\bar{H} \to 0$ for all U. Hence, $\bar{W}/U$ approaches $81\pi/(\bar{H}\sqrt{U})^2$ as $\bar{H}\sqrt{U} \to 0$

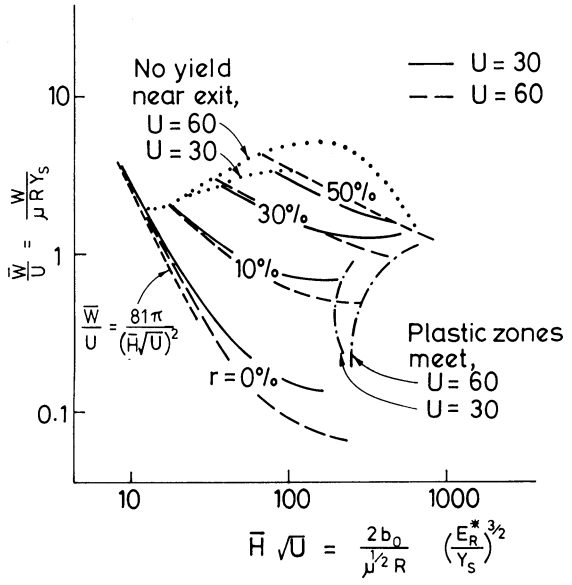

FIG. 5. Effect of inlet strip thickness and reduction on rolling load.

for all U. This suggests that the correct way to combine $\bar{W}$, $\bar{H}$ and U is in the form $\bar{W}/U$ and $\bar{H}\sqrt{U}$. It is clear from Fig. 5 that $\bar{W}/U$ is strongly dependent upon $\bar{H}\sqrt{U}$ and r, and little influenced by U. Similarly, the rolling torque $\bar{Q}/U$ is sensitive to $\bar{H}\sqrt{U}$ and r, and only weakly dependent upon U, as shown in Fig. 6.

Consider the predicted rolling torque, $\bar{Q}$, in more detail. When r is zero, the pressure distribution is symmetrical about the centre-line through the roll centres and $\bar{Q}$ is zero. When $\bar{H}\sqrt{U}$ is less than about 100, $\bar{Q}$ increases to a maximum with increasing r and then decreases again, see Fig. 6. At higher values of $\bar{H}\sqrt{U}$, $\bar{Q}$ increases monotonically with increasing r, and the new theory gives similar predictions to those of the Bland and Ford model [3]. This agreement with the Bland and Ford model is due to the fact that at high $\bar{H}\sqrt{U}$ the two models predict similar deformations of the strip.

The slip velocities predicted by the new theory are given in Fig. 7. It is apparent that the slips $(v_S - v_R)/V_R$ at entry and at exit are strong functions of r, and weaker functions of $\bar{H}\sqrt{U}$ and U. Always, the slip at entry is greater in magnitude than at exit, reflecting the fact that greater plastic reduction occurs at entry than at exit.

Consider the effect of varying $\bar{H}\sqrt{U}$ on the slip at exit for fixed values of r and U, Fig. 7. As $\bar{H}\sqrt{U}$ decreases the slip at exit drops to zero when there is no longer a yield zone at exit. The slip at exit also decays towards zero at large $\bar{H}\sqrt{U}$. This happens when the plastic zone B extends to the exit.

The slips at entry and exit are compared with the Bland and Ford solution [3] in Fig. 8, for the case $U = 30$. There is good agreement between the two models, implying that they predict

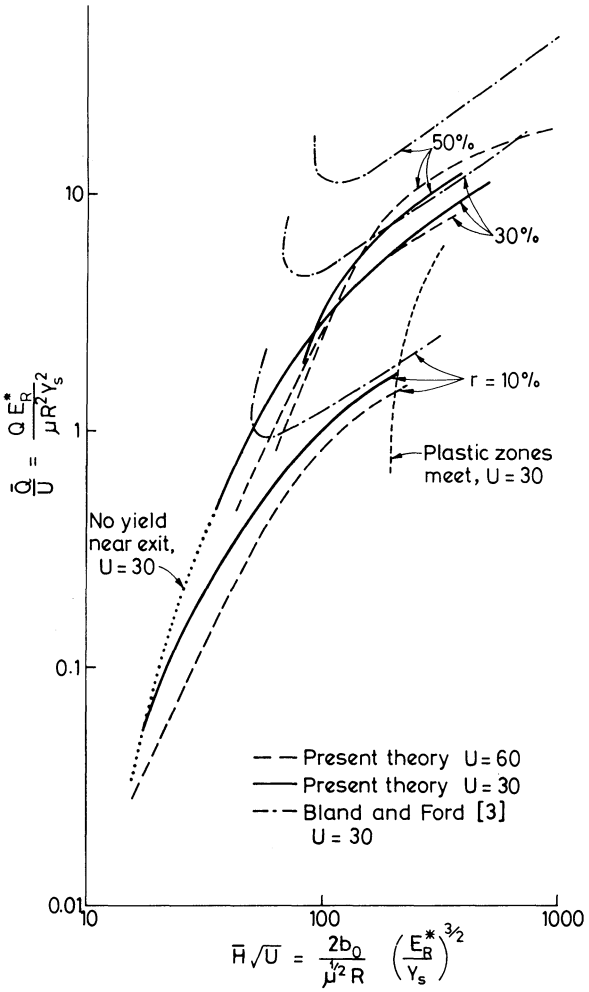

FIG. 6. Comparison of rolling torque predicted by new theory and by Bland and Ford [3].

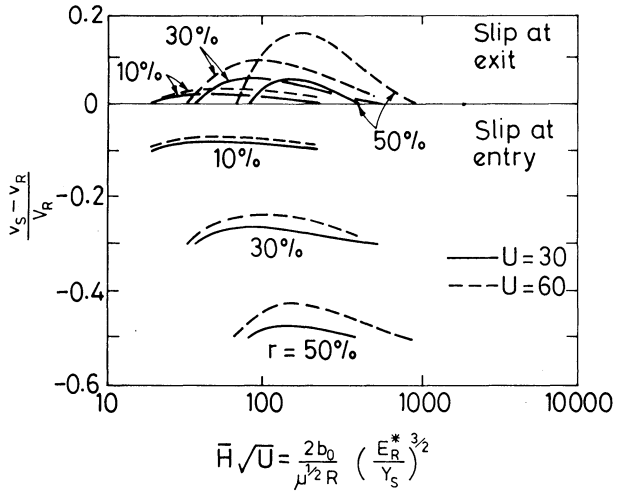

FIG. 7. Slip of strip relative to work rolls at entry and at exit.

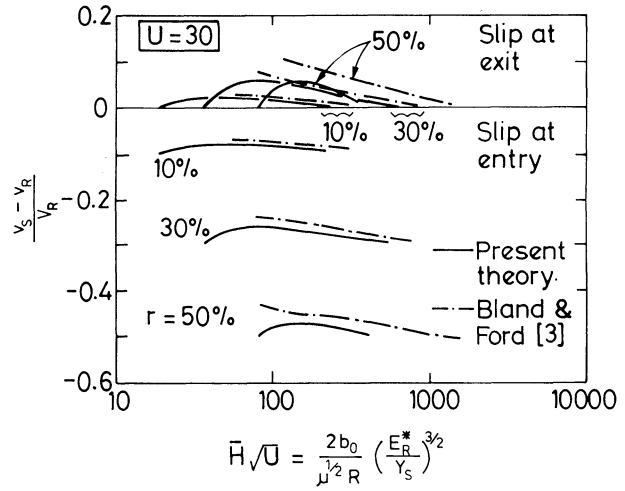

FIG. 8. Comparison of slip behaviour predicted by new theory and by Bland and Ford [3].

similar proportions of plastic reduction near entry and near exit. This agreement over a wide range of $\bar{H}\sqrt{U}$ is probably fortuitous.

8. CONCLUDING DISCUSSION

A new theoretical framework has been developed with which to analyse the foil rolling problem. The analysis suggests that a neutral region of no-slip exists in the roll bite, for finite reductions of the strip. This was suggested by Johnson and Bentall [5] for the case of zero reduction. Previous theories of strip rolling, such as the Bland and Ford solution [3], assume full slip throughout the contact region and predict incorrectly the existence of a limiting gauge. For the case of thick strip, the new theory and the Bland and Ford model suggest similar behaviours.

It is thought that the new model provides a physical picture of the foil rolling process which is qualitatively correct. We express caution with regard to the quantitative results, as the location of plastic deformation in the roll bite and the rolling loads and torques are sensitive to the model chosen for deformation of the rolls. A more realistic treatment of the rolls is required in order to determine the accuracy of the present results.

The analysis suggests that more plastic reduction occurs near entry than near exit of the roll bite. If strain hardening of the strip were to be included in the rolling model then the plastic

zone near exit would shrink in size, and an even larger proportion of plastic reduction would occur near entry.

The application of front tension to the strip would increase the size of the plastic zone near exit, while back tension would increase the plastic zone size near entry. Equal front and back tensile stresses effectively reduce the yield stress of the strip by an amount equal to this tension while leaving all other features of the model unchanged.

The model of foil rolling presented here can be modified in a straightforward manner to include strain hardening of the strip and different front and back tensions. Work is in progress to incorporate a more realistic treatment of roll deformation and to determine a more appropriate friction law than the Coulomb law used here.

Acknowledgements—N. A. Fleck wishes to thank Pembroke College and the Maudslay Society for financial support in the form of a research fellowship, when this work was conducted. Both authors are grateful for helpful discussions with Davy McKee (Poole) Ltd.

REFERENCES

1. T. VON KÁRMÁN, Beitrag zür theorie des Walzvorganges. *Z. angew. Math. Mech.* **5**, 139 (1925).
2. E. OROWAN, Graphical calculation of roll pressure with the assumptions of homogeneous compression and slipping friction. *Proc. Inst. Mech. Engrs* **150**, 141 (1943).
3. D. R. BLAND and H. FORD, The calculation of roll force and torque in cold strip rolling with tensions. *Proc. Inst. Mech. Engrs* **159**, 144 (1948).
4. H. FORD and J. M. ALEXANDER, Rolling hard material in thin gauges. Basic considerations. *J. Inst. Metals* **88**, 193 (1959).
5. K. L. JOHNSON and R. H. BENTALL, The onset of yield in the cold rolling of thin strip. *J. Mech. Phys. Solids* **17**, 253 (1969).
6. M. J. GRIMBLE, Solution of the nonlinear functional equations representing the roll gap relationships in a cold mill. *J. Optimization Theor. Applic.* **26** (3), 427 (1978).
7. M. J. GRIMBLE, M. A. FULLER and G. F. BRYANT, A non-circular arc roll force model for cold rolling. *Int. J. Num. Methods Engng* **12**, 643 (1978).
8. Z. QUAN, Deformation characteristics of the cross shear cold rolling (CSCR) of ultra thin strip and the theory of the "Elastic Plug". *Proc. Adv. Technol. Plastic.* **2**, 1173 (1984).
9. K. L. JOHNSON, *Contact Mechanics*. Cambridge University Press, Cambridge (1985).

APPENDIX 1

STRESSES IN STRIP AND SLIP EQUATIONS

First, the indentation condition is considered in order to determine a_2/a_0, where a_2 is the contact size at exit and a_0 is the contact size at entry, defined in Fig. 2.

The normal pressure distribution has already been given by

$$p(x) = p_0\sqrt{1-(x/a_0)^2} - K_p\Delta b, \tag{3}$$

where $2\Delta b$ is the reduction of strip thickness. The maximum Hertzian pressure $p_0 = E^*_R a_0/2R$ may be expressed in dimensionless form as,

$$\frac{p_0}{Y_s} = U\frac{a_0}{2\mu R}, \tag{A1}$$

where $U = \mu E^*_R/Y_S$.

The contact size at exit a_2 may be related to the contact size at entry a_0 by substituting into equation (3a) the condition that $p = 0$ and $\Delta b = \Delta b_2 = rb_0$ at $x = a_2$. This gives,

$$\left(\frac{a_2}{a_0}\right)^2 = 1-\left(\frac{a_0K_p}{E^*_R}\frac{2\mu R}{a_0}\frac{b_0}{\mu a_0}r\right)^2. \tag{A2}$$

Here $r = (b_0 - b_2)/b_0 = \Delta b_2/b_0$ is the overall reduction of the strip.

The strip thickness, $2b_1$, in the central zones C, D and E equals $2b_0 - 2\Delta b_1$, where $2\Delta b_1$ is the reduction of strip thickness due to passage of the strip through the plastic zone B. The intermediate reduction, r_1, defined by

$$r_1 = \frac{b_1 - b_2}{b_1} \tag{A3}$$

is related to Δb_1 by,

$$\Delta b_1 = b_0 - b_1 = b_0\left(1-\frac{1-r}{1-r_1}\right). \tag{A4}$$

Equations are now given for the stresses in the strip and the slip distribution in each of the deformation zones A–G. Stresses are defined in terms of the cartesian co-ordinates x, z, shown in Fig. 1(a).

Zone A (refer to Fig. 2)

In zone A, the strip is elastic and has a lower velocity than the work rolls. Elastic compression of the strip is neglected in the thickness, z direction. By equation (3a), the strip experiences a normal stress σ_z of

$$\frac{-\sigma_z}{p_0} = \frac{p}{p_0} = \sqrt{1-(x/a_0)^2} \tag{A5}$$

and a shear stress $q = \mu p$, so that

$$\frac{q}{\mu p_0} = \frac{p}{p_0} = \sqrt{1-(x/a_0)^2}. \tag{A6}$$

The longitudinal stress σ_x is derived by integrating the equilibrium equation (2) with the assumption $db/dx = 0$, giving

$$\frac{-\sigma_x}{p_0} = \frac{1}{2}\frac{\mu a_0}{b_0}\left[\frac{x}{a_0}\sqrt{1-(x/a_0)^2} + \sin^{-1}\frac{x}{a_0} + \pi/2\right]. \tag{A7}$$

Zone B

The strip experiences plastic reduction and slips relative to the work rolls. The yield condition gives,

$$\frac{\sigma_x}{p_0} = \frac{\sigma_z}{p_0} + \frac{Y_S}{p_0} \tag{A8}$$

and the slip condition gives

$$\frac{q}{\mu p_0} = \frac{p}{p_0} = -\frac{\sigma_z}{p_0}. \tag{A9}$$

The pressure gradient, $-d\sigma_z/dx$, is derived from equations (A1), (A8) and (A9) and the equilibrium equation (2). We obtain,

$$-\frac{d(\sigma_z/p_0)}{d(x/a_0)} = \frac{-\left(\frac{\sigma_z}{p_0}\right) + \frac{1}{U}\frac{E_R^*}{a_0 K_p}\frac{x/a_0}{\sqrt{1-(x/a_0)^2}}}{\frac{b_0}{\mu a_0} - \frac{E_R^*}{a_0 K_p}\frac{a_0}{2\mu R}\sqrt{1-\left(\frac{x}{a_0}\right)^2} - \frac{E_R^*}{a_0 K_p}\frac{a_0}{2\mu R}\frac{\sigma_z}{p_0} - \frac{1}{U}\frac{E_R^*}{a_0 K_p}}. \tag{A10}$$

The pressure distribution $-\sigma_z$ is determined by integrating equation (A10) from the boundary of zone A using the Runge–Kutta numerical procedure. The stresses σ_x and q then follow directly from equations (A8) and (A9).

The strip thickness $2b$ at any location is calculated by equating the normal pressure distribution $-\sigma_z$ to the formula (3a) governing roll deformation. Thus,

$$\frac{b}{\mu a_0} = \frac{b_0}{\mu a_0} - \frac{E_R^*}{a_0 K_p}\frac{a_0}{2\mu R}\sqrt{1-\left(\frac{x}{a_0}\right)^2} - \frac{E_R^*}{a_0 K_p}\frac{a_0}{2\mu R}\frac{\sigma_z}{p_0}. \tag{A11}$$

We calculate the slip distributions $(v_S - v_R)/V_R$ throughout the contact region from the distribution of plastic strain in the strip. The contribution to slip from the elastic longitudinal strains in the strip and rolls is neglected in our presentation of slip behaviour. This is reasonable, since the elastic strains are usually much less than the plastic reduction of the strip.

Thus, the slip distribution $(v_S - v_R)/V_R$ in zone B is determined with the aid of the continuity equation $v_S b = V_R b_1$, and equation (A4), giving

$$\frac{v_S - v_R}{V_R} = \frac{1-r}{1-r_1}\frac{b_0}{\mu a_0}\frac{\mu a_0}{b} - 1. \tag{A12}$$

An explicit expression for $(v_S - v_R)/V_R$ is found by substituting equation (A11) into equation (A12).

Zone C

The strip suffers contained plastic deformation with no slip in zone C. The normal pressure is given by equation (3a), with $\Delta b = \Delta b_1$ defined by equation (A4). We obtain,

$$\frac{-\sigma_z}{p_0} = \sqrt{1-(x/a_0)^2} - \left(1 - \frac{1-r}{1-r_1}\right)\frac{b_0}{\mu a_0}\frac{2\mu R}{a_0}\frac{a_0 K_p}{E_R^*}. \tag{A13}$$

The longitudinal stress σ_x is found from equation (A13), using the yield criterion,

$$\frac{\sigma_x}{p_0} = \frac{\sigma_z}{p_0} + \frac{Y_S}{p_0} \tag{A14}$$

and the shear stress q is derived from equations (2), (A13) and (A14) and the assumption that $db/dx = 0$. Thus,

$$\frac{q}{\mu p_0} = -\left(\frac{1-r}{1-r_1}\right)\frac{b_0}{\mu a_0}\frac{x/a_0}{\sqrt{1-(x/a_0)^2}}. \tag{A15}$$

Zone D

The strip behaves elastically and experiences no slip with respect to the work rolls.

The normal stress σ_z is given by equation (A13), while σ_x and q are found from the no slip condition and from the equilibrium equation, as follows.

For the case of no-slip, equation (8) reduces to

$$0 = (\varepsilon_x)_S - (\varepsilon_x)_R + \xi, \tag{A16}$$

where the creep ratio, ξ, is an unknown constant determined by the analysis. For convenience, ξ is defined in terms of the elastically unstrained velocity of the strip in this no-slip zone. Hence, the strain $(\varepsilon_x)_S$ in equation (A16) does not include a plastic component due to plastic reduction which occurs near the entry of the roll bite.

It is assumed that the tangential strain at the surface of the rolls is composed of a shear contribution $du/dx = -(1/K_q)(dq/dx)$, from equation (4) and also of a normal pressure contribution. When an elastic half-space is loaded in plane strain by an arbitrary pressure distribution $p(x)$, a material element at the surface of the half-space suffers a direct stress normal to the surface $\sigma_z = -p$, a direct stress tangential to the surface $\sigma_x = -p$, and no shear stresses. The associated tangential tensile strain ε_x equals $-[(1-2\nu_R)(1+\nu_R)/E_R]p(x)$. Hence, in the present problem the longitudinal strain in the rolls, $(\varepsilon_x)_R$, is assumed to be,

$$(\varepsilon_x)_R = -\frac{1}{K_q}\frac{dq}{dx} - \frac{(1-2\nu_R)(1+\nu_R)}{E_R}p(x). \tag{A17}$$

The longitudinal strain in the strip $(\varepsilon_x)_S$ is,

$$(\varepsilon_x)_S = \frac{1-\nu_S^2}{E_S}\sigma_x - \frac{\nu_S(1+\nu_S)}{E_S}\sigma_z. \tag{A18}$$

Equations (A4) and (A16)–(A18) may be combined with the equilibrium equation (2) and the assumption that $db/dx = 0$ to give,

$$\frac{b_0}{K_q}\frac{1-r}{1-r_1}\frac{d^2\sigma_x}{dx^2} - \frac{\sigma_x}{E_S^*} = \xi - \frac{\sigma_z}{E'}, \tag{A19}$$

where

$$\frac{1}{E'} = \frac{(1-2\nu_R)(1+\nu_R)}{E_R} + \frac{\nu_S(1+\nu_S)}{E_S}. \tag{A20}$$

We can reduce equations (A13) and (A19) to a dimensionless, second-order differential equation,

$$\frac{d^2(\sigma_x/p_0)}{d(x/a_0)^2} - \gamma^2\frac{\sigma_x}{p_0} = \frac{1-r_1}{1-r}\frac{a_0K_q}{E_R^*}\frac{2R\xi}{b_0} + \frac{E_S^*}{E'}\frac{E_R^*}{\mu E_S^*}\frac{a_0K_q}{E_R^*}\frac{1-r_1}{1-r}\frac{\mu a_0}{b_0}\left[\sqrt{1-\left(\frac{x}{a_0}\right)^2} - \left(1-\frac{1-r}{1-r_1}\right)\frac{b_0}{\mu a_0}\frac{2\mu R}{a_0}\frac{a_0K_p}{E_R^*}\right], \tag{A21}$$

where

$$\gamma^2 = \frac{1-r_1}{1-r}\frac{a_0K_q}{E_R^*}\frac{E_R^*}{\mu E_S^*}\frac{\mu a_0}{b_0}. \tag{A22}$$

In order to find the particular integral of this differential equation the term $\sqrt{1-(x/a_0)^2}$ on the right-hand side is expanded as a power series. The solution of the differential equation to within a few per cent is,

$$\frac{-\sigma_x}{p_0} = L_3 + L_4\exp\left(\frac{\gamma x}{a_0}\right) + L_5\exp\left(-\frac{\gamma x}{a_0}\right) - \frac{E_R^*}{\mu E_S^*}\frac{E_S^*}{E'}\frac{\mu a_0}{b_0}\frac{a_0K_q}{E_R^*}\frac{1-r_1}{1-r}\left[\alpha_3 + \alpha_4\left(\frac{x}{a_0}\right)^2 + \alpha_5\left(\frac{x}{a_0}\right)^4 + \alpha_6\left(\frac{x}{a_0}\right)^6\right], \tag{A23}$$

where L_4 and L_5 are unknown constants and,

$$\begin{aligned}
L_3 &= \frac{1}{\gamma^2}\frac{1-r_1}{1-r}\frac{a_0K_q}{E_R^*}\frac{2R\xi}{b_0} - \frac{E_S^*}{E'}\frac{a_0K_p}{E_R^*}\frac{2\mu R}{a_0}\frac{b_0}{\mu a_0}\left(1-\frac{1-r}{1-r_1}\right)\\
\alpha_3 &= \frac{45}{\gamma^8} + \frac{3}{\gamma^6} + \frac{1}{\gamma^4} - \frac{1}{\gamma^2}\\
\alpha_4 &= \frac{45}{2\gamma^6} + \frac{3}{2\gamma^4} + \frac{1}{2\gamma^2}\\
\alpha_5 &= \frac{15}{8\gamma^4} + \frac{1}{8\gamma^2}\\
\alpha_6 &= \frac{1}{16\gamma^2}.
\end{aligned} \tag{A24}$$

The interfacial shear stress q is deduced from σ_x via the equilibrium equation (2), giving

$$\frac{q}{\mu p_0} = \frac{1-r}{1-r_1}\frac{b_0}{\mu a_0}\gamma\left(L_4 \exp\left(\frac{\gamma x}{a_0}\right) - L_5 \exp\left(-\frac{\gamma x}{a_0}\right)\right) - \frac{E_R^*}{\mu E_S^*}\frac{E_S^*}{E'}\frac{a_0 K_q}{E_R^*}\left[2\alpha_4\left(\frac{x}{a_0}\right) + 4\alpha_5\left(\frac{x}{a_0}\right)^3 + 6\alpha_6\left(\frac{x}{a_0}\right)^5\right]. \tag{A25}$$

Zone E

In zone E, the strip behaves elastically and travels more quickly than the work rolls.

The normal pressure on the strip $-\sigma_z$ is given by equation (A13), and the interfacial shear stress q is

$$\frac{q}{\mu p_0} = -\frac{p}{p_0} = \frac{\sigma_z}{p_0}. \tag{A26}$$

We integrate the equilibrium equation (2) using equation (A26) and the assumption that $db/dx = 0$ in order to determine the longitudinal stress σ_x,

$$\frac{\sigma_x}{p_0} = \frac{1}{2}\frac{\mu a_0}{b_0}\frac{1-r_1}{1-r}\left[\frac{x}{a_0}\sqrt{1-\left(\frac{x}{a_0}\right)^2} + \sin^{-1}\frac{x}{a_0}\right] - \left(\frac{1-r_1}{1-r} - 1\right)\frac{2\mu R}{a_0}\frac{a_0 K_p}{E_R^*}\frac{x}{a_0} + L_6, \tag{A27}$$

where L_6 is an arbitrary constant of integration.

Zone F

The strip experiences plastic reduction and has a greater velocity than the work rolls.

The equations governing the stresses and slip distribution are similar to those in zone B with the shear stress q given by equation (A26) rather than equation (A9). The longitudinal stress σ_x is deduced from the yield condition, equation (A8). The pressure gradient $-d\sigma_z/dx$ is derived in an analogous manner to equation (A10), giving

$$-\frac{d(\sigma_z/p_0)}{d(x/a_0)} = \frac{\dfrac{\sigma_z}{p_0} + \dfrac{1}{U}\dfrac{E_R^*}{a_0 K_p}\dfrac{x/a_0}{\sqrt{1-(x/a_0)^2}}}{\dfrac{b_0}{\mu a_0} - \dfrac{E_R^*}{a_0 K_p}\dfrac{a_0}{2\mu R}\sqrt{1-\left(\dfrac{x}{a_0}\right)^2} - \dfrac{E_R^*}{a_0 K_p}\dfrac{a_0}{2\mu R}\dfrac{\sigma_z}{p_0} - \dfrac{1}{U}\dfrac{E_R^*}{a_0 K_p}}. \tag{A28}$$

We determine $-\sigma_z$ by integrating equation (A28) numerically with respect to decreasing x from the boundary of zone G, using the Runge–Kutta procedure.

The slip velocity of the strip relative to the rolls is calculated using equations (A11) and (A12), as before.

Zone G

The strip suffers elastic unloading and travels faster than the rolls in the final zone, G.

We compute the normal pressure $-\sigma_z$ from equation (3a) which governs deformation of the rolls, and the condition that $\Delta b = rb_0$ for the strip, hence

$$\frac{-\sigma_z}{p_0} = \sqrt{1-\left(\frac{x}{a_0}\right)^2} - r\frac{b_0}{\mu a_0}\frac{2\mu R}{a_0}\frac{a_0 K_p}{E_R^*}. \tag{A29}$$

The interfacial shear stress q is given by equation (A26), and the longitudinal stress σ_x is deduced by integration of the equilibrium equation (2) with the condition that $b = b_2 = (1-r)b_0$, giving

$$\frac{-\sigma_x}{p_0} = -\frac{1}{2}\frac{\mu a_0}{b_0}\frac{1}{1-r}\left[\frac{x}{a_0}\sqrt{1-\left(\frac{x}{a_0}\right)^2} + \sin^{-1}\left(\frac{x}{a_0}\right)\right] + \frac{r}{1-r}\frac{2\mu R}{a_0}\frac{a_0 K_p}{E_R^*}\frac{x}{a_0} + L_7, \tag{A30}$$

where L_7 is an arbitrary constant of integration.

APPENDIX 2

METHOD OF SOLUTION

The pressure distribution, $-\sigma_z$, rolling load and torque, and slip distribution associated with plastic reduction are functions only of $\mu a_0/b_0$, r and $U = \mu E_R^*/Y_S$. If the stress distributions σ_x and q are required in the central elastic, no slip zone D, then two further non-dimensional groups $\mu E_S^*/E_R^*$ and E_S^*/E' are required. In this study $\mu E_S^*/E_R^*$ and E_S^*/E' are given the values of 0.01 and 0.683, respectively; these are typical values for foil rolling of aluminium and its alloys with steel work rolls. The non-dimensional groups $a_0 K_p/E_R^*$ and $a_0 K_q/E_R^*$ are assumed to equal $8/3\pi$ and $16/9\pi$, respectively, as discussed in Section 3.2.

Consider the general case of a finite reduction r, with $\mu a_0/b_0$, U, $\mu E_S^*/E_R^*$ and E_S^*/E' given. The stresses in the roll bite are found as follows.

Calculation of stresses

An iterative procedure is used to deduce p_0/Y_S, $a_0/\mu R$ and a_2/a_0. From an initial guessed value of p_0/Y_S of unity, $a_0/\mu R$ is calculated from equation (A1), and a_2/a_0 from equation (A2). A new value for p_0/Y_S is found from the

condition that $\sigma_x - \sigma_z = Y_S$ at the boundary of zone G with zone F. Denote the location of this boundary by x_F. Then, equations (A29) and (A30) for the stresses in the elastic zone G give,

$$\frac{Y_S}{p_0} = \frac{\sigma_x}{p_0} - \frac{\sigma_z}{p_0} = \sqrt{1-(x_F/a_0)^2} - r\frac{b_0}{\mu a_0}\frac{2\mu R}{a_0}\frac{a_0 K_p}{E_R^*} + \frac{1}{2}\frac{1}{1-r}\frac{\mu a_0}{b_0}\left[\frac{x_F}{a_0}\sqrt{1-(x_F/a_0)^2} + \sin^{-1}\frac{x_F}{a_0}\right] - \frac{r}{1-r}\frac{2\mu R}{a_0}\frac{a_0 K_p}{E_R^*}\frac{x_F}{a_0} - L_7, \tag{B1}$$

where L_7 is deduced from equation (A30) and the boundary condition $\sigma_x = 0$ at $x = a_2$,

$$L_7 = \frac{1}{2}\frac{1}{1-r}\frac{\mu a_0}{b_0}\left[\frac{a_2}{a_0}\sqrt{1-(a_2/a_0)^2} + \sin^{-1}\frac{a_2}{a_0}\right] - \frac{r}{1-r}\frac{2\mu R}{a_0}\frac{a_0 K_p}{E_R^*}\frac{a_2}{a_0}. \tag{B2}$$

In order to calculate p_0/Y_S from equations (B1) and (B2) x_F is determined, as follows.

At the end of the plastic zone F, x equals x_F, db/dx equals zero and q is continuous. Equation (2) implies that $d\sigma_x/dx$ is continuous and equation (3a) that $d\sigma_z/dx$ is continuous. Since $\sigma_x - \sigma_z = Y_S$ throughout zone F, we deduce that $d(\sigma_x - \sigma_z)/dx$ equals zero throughout zone F. By continuity, $d(\sigma_x - \sigma_z)/dx$ equals zero in the elastic zone G at $x = x_F$. Substitution of equations (A29) and (A30) into the condition that $d(\sigma_x - \sigma_z)/dx = 0$ at $x = x_F$ leads to,

$$\frac{1}{1-r}\frac{\mu a_0}{b_0}\left(1-\left(\frac{x_F}{a_0}\right)^2\right) - \frac{x_F}{a_0} - \frac{r}{1-r}\frac{2\mu R}{a_0}\frac{a_0 K_p}{E_R^*}\sqrt{1-(x_F/a_0)^2} = 0. \tag{B3}$$

Equation (B3) is solved by the Newton–Raphson method in order to determine x_F and p_0/Y_S is calculated from equations (B1) and (B2).

From this improved estimate of p_0/Y_S corresponding values of $a_0/\mu R$ and a_2/a_0 are computed via equations (A1) and (A2), respectively. The above procedure to find p_0/Y_S is then repeated until sufficient accuracy is attained.

Next, the boundary $x = x_A$ between zones A and B is calculated from the condition that yield occurs at the end of the elastic zone A. Substitution of equations (A5) and (A7) into the yield criterion $\sigma_x - \sigma_z = Y_S$ leads to

$$\sqrt{1-\left(\frac{x_A}{a_0}\right)^2} - \frac{1}{2}\frac{\mu a_0}{b_0}\left[\frac{x_A}{a_0}\sqrt{1-\left(\frac{x_A}{a_0}\right)^2} + \sin^{-1}\left(\frac{x_A}{a_0}\right) + \frac{\pi}{2}\right] - \frac{Y_S}{p_0} = 0. \tag{B4}$$

We solve for x_A/a_0 by the Newton–Raphson method.

The end of the plastic zone B, $x = x_B$, is determined by integrating equation (A10) through the plastic zone by the Runge–Kutta method, until $db/dx = 0$. This condition may be rewritten in terms of $d\sigma_z/dx$ with the aid of equation (3a), giving

$$\left(\frac{d(\sigma_z/p_0)}{d(x/a_0)}\right)_{x=x_B} = \frac{x_B/a_0}{\sqrt{1-(x_B/a_0)^2}}. \tag{B5}$$

We calculate the intermediate reduction, $r_1 = (b_1 - b_2)/b_1$, by matching the known pressure $-\sigma_z$ at $x = x_B$ with the pressure distribution in zone C, equation (A13).

In order to compute the stress distribution in the elastic zones D and E, we first determine the pressure distribution in the plastic reduction zone F. Equation (A28) is integrated numerically with respect to decreasing x from the known conditions at $x = x_F$. The start of the plastic zone F at $x = x_E$ is deduced from the point of intersection of the integrated pressure curve in zone F and the pressure distribution in zone E, equation (A13). Continuity of σ_x at $x = x_E$ is used to find L_6 in equation (A27). The stresses in region E are then fully specified.

Last, we determine the stresses in zone D, and the locations of its boundaries with zones C and E, $x = x_C$ and $x = x_D$, respectively. The boundary conditions at both x_C and x_D are continuity of q and σ_x. Also, we have continuity of dq/dx at x_C in order to satisfy continuity of no-slip; this is deduced from equations (A16)–(A18). These five boundary conditions are used to solve for the five unknowns L_3, L_4 and L_5 in equations (A23) and (A25), and x_C and x_D using an iterative method.

Calculation of $\bar{H}$, $\bar{W}$, $\bar{Q}$ *and* $(v_S - v_R)/V_R$

The dependent variables $\bar{H}$, $\bar{W}$ and $\bar{Q}$ and the slip distribution $(v_S - v_R)V_R$ are calculated from the independent groups r, $\mu a_0/b_0$, and U as follows.

The non-dimensional inlet strip thickness, $\bar{H}$, can be expressed in terms of $b_0/\mu a_0$ and p_0/Y_S,

$$\bar{H} = \frac{2b_0 E_R^*}{\mu R Y_S} = 4\frac{b_0}{\mu a_0}\frac{p_0}{Y_S} \tag{B6}$$

with the aid of equation (A1). Here, p_0/Y_S is known for any set of values of r, $\mu a_0/b_0$ and U.

The rolling load, W, is found by integrating the pressure $p(x)$ over the contact region, as defined in equation (9). With the aid of equation (A1), this may be re-expressed in non-dimensional terms as,

$$\bar{W} = \frac{WE_R^*}{RY_S^2} = 2\left(\frac{p_0}{Y_S}\right)^2 \int_{-1}^{a_2/a_0} \frac{-\sigma_z}{p_0}\, d\left(\frac{x}{a_0}\right). \tag{B7}$$

Thus $\bar{W}$ may be found for a given r, $\mu a_0/b_0$ and U. The integral of equation (B7) is evaluated numerically by Simpson's rule for the plastic zones B and F. Analytical expressions are derived for the other zones.

The rolling torque per work roll, $\bar{Q}$, is determined by integrating the moment of the roll pressure about the point $x = 0$, equation (10). We obtain the non-dimensional rolling torque $\bar{Q}$ by combining equations (10) and (A1),

$$\bar{Q} = \frac{QE_R^{*2}}{R^2 Y_S^3} = 4\left(\frac{p_0}{Y_S}\right)^3 \int_{-1}^{a_2/a_0} \frac{\sigma_z}{p_0} \frac{x}{a_0} \, \mathrm{d}\left(\frac{x}{a_0}\right). \tag{B8}$$

The contribution to the integral of equation (B8) from the plastic zones B and F is determined numerically using Simpson's rule. Analytical expressions are derived for the contribution to the integral from the other zones.

The slip distribution $(v_S - v_R)/V_R$ in zones B and F is given by equation (A12), with the aid of equation (A11). By conservation of mass flow rate, the slip at entry $((v_S - v_R)/V_R)_{entry}$, and at exit $((v_S - v_R)/V_R)_{exit}$ can be expressed in terms of r and r_1 alone,

$$\left(\frac{v_S - v_R}{V_R}\right)_{entry} = \frac{1-r}{1-r_1} - 1 \tag{B9a}$$

and

$$\left(\frac{v_S - v_R}{V_R}\right)_{exit} = \frac{1}{1-r_1} - 1. \tag{B9b}$$

The intermediate reduction, r_1, is known for given values of r, $\mu a_0/b_0$ and U.